

2.3 A SIMPLE PARAMETERIZATION FOR DETRAINMENT IN SHALLOW CUMULUS

Wim C. de Rooy* and A. Pier Siebesma
Royal Netherlands Meteorological Institute, The Netherlands

1. INTRODUCTION

Recently there has been a regained interest in the parameterization for entrainment in cumulus convection (Siebesma and Cuijpers 1995, Siebesma 1998, Grant and Brown 1999, Neggers et al. 2002). However, little attention has been paid to the parameterization of the detrainment process although this counterpart of the cloud mixing process is equally important for obtaining realistic mass flux profiles in cumulus convection.

The most simple, and still widely applied, description of lateral mixing in a mass flux concept is the use of constant fractional entrainment (ϵ) and detrainment (δ) rates. As we will demonstrate in this study there are at least two disadvantages to such an approach. Firstly, the dependency of detrainment rate on the cloud layer depth is ignored. Secondly, the use of constant entrainment and detrainment rates results into an insensitivity to changes in the humidity of the environment of the convective updrafts (Kain and Fritsch 1990). Therefore, Kain and Fritsch (1990) introduced a buoyancy sorting concept in convection schemes. Although physically appealing, this concept uses difficult to determine functions and tunable parameters. Moreover, buoyancy sorting convection schemes show some unwanted characteristics (Jonker 2005).

In this paper we propose a simple but flexible parameterization for the detrainment process that addresses the two aforementioned shortcomings. This parameterization shows the right sensitivity to cloud height and environmental conditions for a wide range of shallow cumulus convection cases.

2. MODELS

2.1 The LES model

A number of Large Eddy Simulation (LES) Model intercomparison studies have shown that these models are well capable of representing the dynamics of the cumulus topped boundary layer (Stevens et al. 2001, Brown et al. 2002, Siebesma et al. 2003). In this paper we will consider the results of the Dutch Atmospheric LES model DALES (Cuijpers and Duynkerke 1993) as pseudo observations.

2.2 The Single Column Model (SCM)

The SCM that will be used is derived from a recent Hirlam NWP model version (Uden 2002). The radiation, dynamical tendencies, and the surface fluxes are prescribed for all cases. Starting point for the used convection scheme is the one developed by Tiedtke (1989) which is used operational at the ECMWF. By using state of the art physical parameterization schemes, the timing of the convective activity and the mass flux at cloud base are in good agreement with the LES results. Also, no rain is produced in the SCM. Therefore, discrepancies in the cloud layer between SCM and LES results can be mainly ascribed to differences in the lateral mixing processes in the convection scheme. As a starting point we adopt the detrainment and entrainment rates according to Siebesma and Cuijpers (1995, henceforth SC95) and Siebesma et al. (2003) respectively (i.e. $\delta=2.75 \times 10^{-3}$ and $\epsilon=1/z \text{ m}^{-1}$). The SCM has 60 layers in the vertical with an effective resolution of around 100 m in the cloud layer.

3. RESULTS

Siebesma and Holtslag (1996) demonstrated that well-chosen constant detrainment and entrainment rates (like the default ones in our SCM) are adequate for the rela-

*Corresponding author address: Wim C. de Rooy, KNMI, P.O. Box 201, 3730 AE, De Bilt, The Netherlands. E-mail: rooyde@knmi.nl

tively simple steady-state BOMEX shallow convection case (Holland and Rasmusen 1973). However, what are the results for a more complex case of a daily cycle of shallow cumulus clouds above land? (ARM, see Brown et al. 2002) In the ARM case cumulus clouds start to develop from approximately 1500 UTC. From then on the cloud base and cloud top rises until about 2130 UTC when the cloud height starts to decrease. Finally at 2430 UTC all clouds collapse, all in agreement with observations. For different simulation times Figs. 1 and 2 show the total specific humidity profiles of the LES model and the SCM respectively.

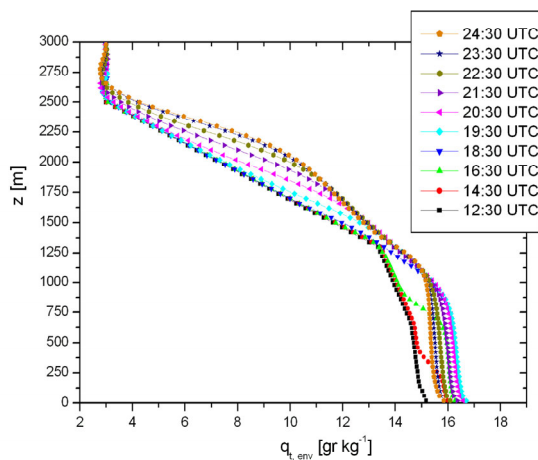


Fig. 1. Total specific humidity profiles for different simulation hours during the ARM case for the LES model.

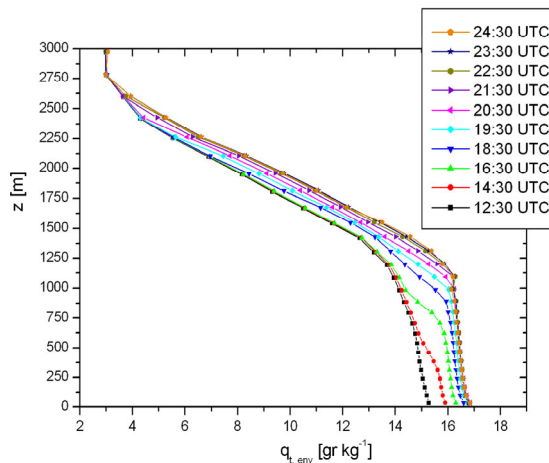


Fig. 2. As Fig.1 but now for the SCM.

Apparently, the convection in the LES model is more active leading to more humidity in the upper half of the cloud layer and less humidity

near cloud base. This is also reflected in the sub cloud layer which, first moistens but becomes drier (in the LES model) when the convection is well developed. To explain these differences between LES model and SCM we first will have to take a closer look to the lateral exchange in the LES model.

If we diagnose the entrainment and detrainment rates in the LES model for this case (not shown), it appears that the absolute and relative differences between the simulation times are much larger for the fractional detrainment rates than for the fractional entrainment rates. This is one of the reasons why we choose to develop a detrainment formulation to produce the correct mass flux profile. Figure 3 presents the dependence of the mean detrainment rate (averaged over the cloud layer) on the cloud height. Most striking is the decrease of δ with increasing cloud height. This can be explained as follows. Many studies considering shallow convection (e.g. SC95) showed that δ is larger than ϵ . Consequently, the mass flux profile decreases with height, reflecting an ensemble of clouds with shallow clouds losing their mass at relatively low heights, and larger clouds transporting mass in the upper part of the cloud layer (SC95). Constant entrainment and detrainment rates, e.g. the ones in our SCM, fix the mass loss per meter. In fact it is the difference between ϵ and δ (see eq. (1)) that determines how fast the mass flux decreases with height and the diagnosed values from SC95 are such that the mass flux profile decreases monotonically to zero for a cloud depth of 1000 m, i.e. the cloud depth observed during BOMEX. However a bold application of these rates on a shallower cloud layer will result in a nonzero mass flux at cloud top while applying these rates on a deeper cloud layer will result in a zero mass flux in the upper part of the cloud layer, all in disagreement with observations. The remedy to this unwanted behavior is also clear; the difference between the entrainment and the detrainment needs to be chosen such that the resulting mass flux is exhausted around cloud top. This calls for smaller detrainment rates for deeper cloud layer, a suggestion already made in Siebesma (1998), and in agreement with the diagnosed detrainment rates displayed in Fig. 3.

A second interesting phenomenon that can be observed in Fig. 3 is that after simulation hour 9 the cloud height decreases without an increase in detrainment. This can be ex-

plained by the fact that for these hours the clouds rise in an environment that is already premoistened for several hours by detrainment from former clouds. Therefore the entrained air will be moister and hence less evaporative cooling will occur resulting in lower detrainment rates than in a dryer environment. This effect has been demonstrated recently in great detail by Derbyshire et. al. (2004) where they studied convective activity in a number of cases in which only the environmental relative humidity was varied. A good measure of this effect can be expressed by the critical fraction of environmental air, χ_c (Kain and Fritsch 1990). This is the fraction of environmental air that is necessary to make the cloud air just neutrally buoyant. Moistening the environmental air will lead to higher χ_c values and smaller detrainment rates. The analytically determined mean critical fractions, $\overline{\chi_c}$ (averaged over the cloud layer) are also plotted in Figure 3.

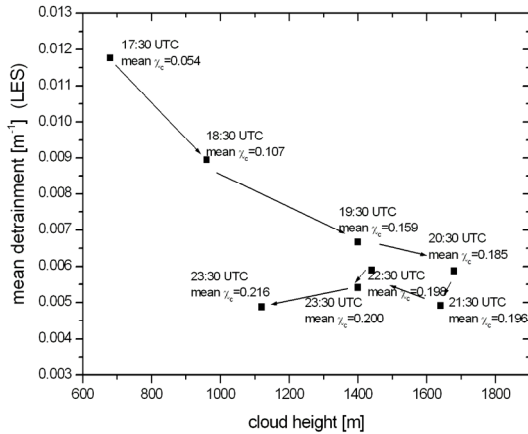
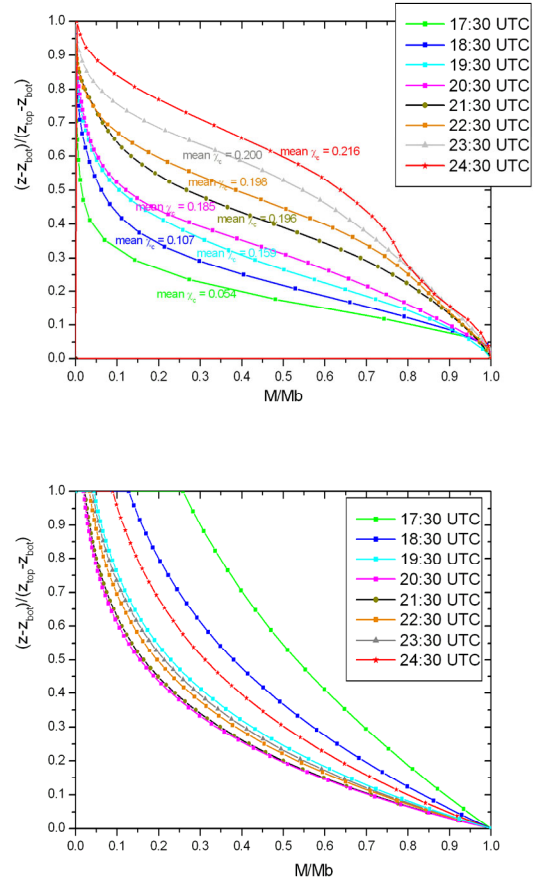


Fig. 3. Mean detrainment rates from the LES model for the ARM case.

To investigate the influence of the environment on the mass flux profile, Figure 4 shows the non-dimensionalized mass flux profile diagnosed from LES results. The mass flux is non-dimensionalized by the mass flux at cloud base Mb while the height is non-dimensionalized by the cloud depth. Note that by re-scaling the height by the cloud depth we already filtered out the effect of cloud depth on the detrainment. If cloud depth would be the only parameter that determined δ , Fig.4 would display a data collapse. Instead we still observe a variation in the shape of the mass flux

profile that is likely due to the different environmental humidity and that correlates well with $\overline{\chi_c}$. Indeed we observe that larger values of $\overline{\chi_c}$ leads to a relatively slower decrease of the mass flux profile and vice versa.

If we use the LES results for Mb, Z_{bot} and Z_{top} but this time apply $\varepsilon=z^{-1}$ and $\delta=0.00275$ (Figure 5), a completely different picture arises. Now the decrease of the non-dimensionalized mass flux profile is determined by the cloud height, leading to large discrepancies with the LES results. For relatively shallow clouds the mass flux does not decrease rapidly enough whereas it decreases too rapidly for the deepest clouds. The latter explains the too inactive convection with the SCM in the second half of the cloudy period of ARM, as discussed for Figure 2.



Figs. 4 and 5. Non-dimensionalized mass flux profiles for different simulations hours (ARM case) of the LES model (upper panel) and for $\varepsilon=z^{-1}$ and $\delta=0.00275$ in combination with Mb, Z_{bot} and Z_{top} from LES (lower panel).

So for an adequate description of the mass flux profile we have to deal with a cloud height as well as (preferably) a χ_c dependence. We start with the continuity of mass equation:

$$\frac{\partial M}{\partial z} = (\varepsilon - \delta)M \quad (1)$$

For ε we simply keep z^{-1} (Siebesma et al. 2003), roughly following the LES results. Note that in our approach the exact formulation of ε is not important for a correct reproduction of the mass flux profile. The detrainment rate is taken constant with height, also roughly according to the LES results (Siebesma et al. 2003). Again, replacing a constant δ with a simple function of z does not influence the results significantly. Now suppose we know the mass flux at an arbitrary height z^* and let us denote the non-dimensionalized mass flux at this height by m^* . Under these assumptions it is straightforward to determine δ and m using (1)

$$\delta = \frac{\ln\left(\frac{z^*}{z_{bot} \cdot m^*}\right)}{(z^* - z_{bot})} \quad (2)$$

$$m = \frac{M(z)}{M_b} = \frac{z}{z_b} \exp(-\delta(z - z_b)) \quad (3)$$

Figure 4 suggests taking z^* half way the cloud because at that height the dependency of m^* on χ_c is most pronounced. Above z^* we impose a linear decrease of the mass flux profile to zero at the cloud top. At first sight this might seem a crude approximation. However, for small m^* there is not much mass flux to spread out anymore and for large m^* the linear decrease seems to be a reasonable approach (see Figure 4). Figure 6 reveals the non-dimensionalized mass flux profile with the new detrainment formulation (2) using the m^* , M_b , z_{bot} and z_{top} as diagnosed by the LES model. Note that with a well chosen constant m^* (e.g. 0.3), the non-dimensionalized mass flux profile is fixed but nevertheless this already results in a large improvement in comparison with constant ε and δ (Figure 5).

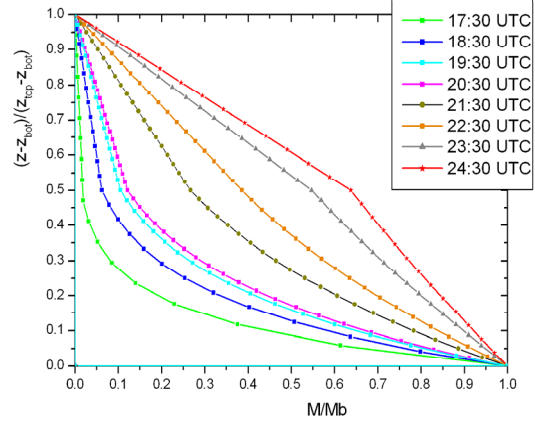


Fig. 6. Non-dimensionalized mass flux profiles for different simulation hours (ARM case) for $\varepsilon=z^{-1}$ and δ according to (2) with M_b , z_{bot} , z_{top} and m^* (half way the cloud) as diagnosed from LES.

One may wonder how generic these results are. Therefore, as an example of another case, we show results for BOMEX. Figures 7 and 8 present the non-dimensionalized mass flux profiles of the LES model and the new detrainment formulation resp. for a few hours in the beginning of the BOMEX period (for spin up reasons we left out the first hour).

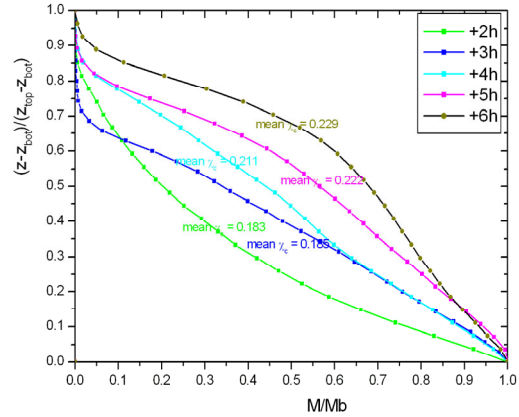


Fig. 7. Non-dimensionalized mass flux profiles for different simulation hours (BOMEX) of the LES model.

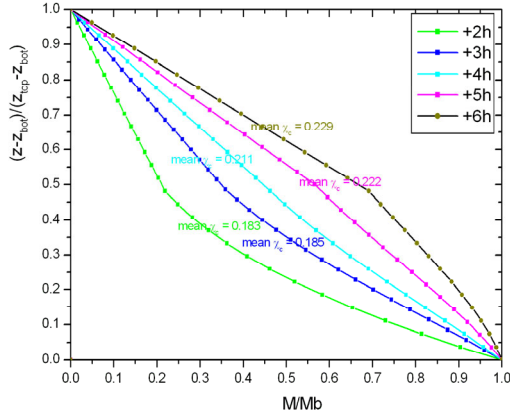


Fig. 8. As Fig. 7 but for $\varepsilon = z^{-1}$ and δ according to (2) with M_b , Z_{bot} , Z_{top} and m^* (half way the cloud) as diagnosed from LES.

Also the results in Figures 7 and 8 are generally in good agreement with our approach. Depending on $\overline{\chi_c}$, m^* values are comparable with the ones from ARM.

Of course the last step that remains to be made is to find a parameterization for m^* in order to close our scheme. Not surprisingly we seek for a correlation between m^* and $\overline{\chi_c}$ in order to parameterize m^* . Figure 9 presents this dependency according to the LES results.

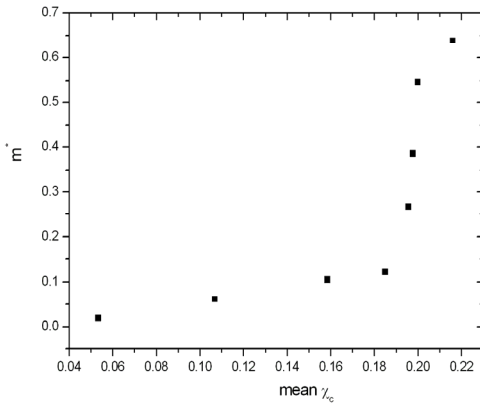


Fig. 9. LES results showing the relation between m^* and $\overline{\chi_c}$.

For the LES results we use the common cloud core definition (see e.g. SC95) to define the cloudy part, which is not exactly comparable with the cloudy updraft in a SCM. As a result,

a relation between m^* and $\overline{\chi_c}$ derived from an LES has to be adapted for use in a SCM. For the moment we have applied:

$$m^* = 5.5 \overline{\chi_c} - 0.17 \quad (4)$$

Figure 10 reveals the total specific humidity profile using (4). The humidity profile is clearly improved. However, although now the sub cloud layer becomes somewhat drier in the second half of the cloudy period, the effect is clearly not strong enough. This might be related to the absence of the cloud height decrease in the SCM during this period. Consequently, $\overline{\chi_c}$ does not increase as much as in the LES model and therefore the convection is less strong, leading to less ventilation of the sub cloud layer.

Note that without the $\overline{\chi_c}$ dependence but with a constant m^* (e.g. 0.3), the humidity profile in Fig. 2 already improves significantly (not shown).

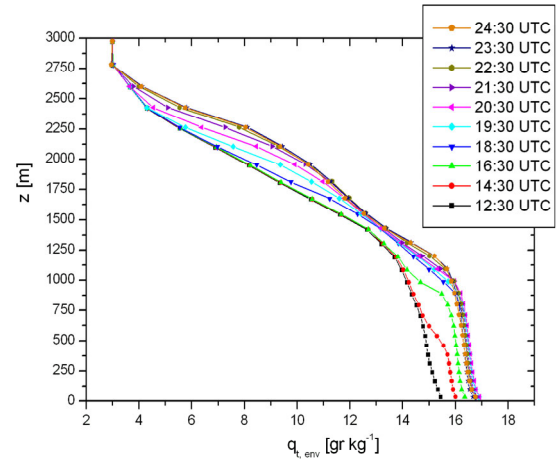


Fig. 10. Total specific humidity profiles for different simulation hours during the ARM case for the SCM using (2) and (4).

4. CONCLUSIONS

A correct simulation of the mass flux profile is very important because it determines the vertical transport of the thermodynamic variables. We demonstrated that one set of constant entrainment and detrainment rates (each with or without height dependence) does not show the correct sensitivity to cloud layer depth, which can result in large deviations from the observed mass flux profile. This can

be remedied using our detrainment formulation in its simplest (one-parameter) form.

For the influence of the cloud environment on the mass flux profile we included a dependence on the bulk critical fraction of environmental air, $\overline{\chi_c}$. With this dependence, the new detrainment parameterization can be seen as an alternative for more complex buoyancy sorting convection schemes. Results from LES and a SCM show the clear potential of our approach for different shallow convection cases.

REFERENCES

- Brown, A.R., et al., 2002: Large-eddy simulation of the diurnal cycle of shallow cumulus convection over land. *Quart. J. Roy. Meteor. Soc.*, **128(B)**, 1075-1094.
- Cuijpers, J.W.M., and P.G. Duynkerke, 1993: Large-eddy simulation of trade-wind cumulus clouds. *J. Atmos. Sci.*, **50**, 3894-3908.
- Derbyshire, S.H., et al., 2004: Sensitivity of moist convection to environmental humidity. *Quart. J. Roy. Meteor. Soc.*, **128**, 1-26.
- Grant, A.L.M., and A.R. Brown, 1999: A similarity hypothesis for shallow cumulus transports. *Quart. J. Roy. Meteor. Soc.*, **125**, 1913-1936.
- Jonker, S., 2005: Evaluation study of the Kain Fritsch convection scheme. KNMI Technical Report, TR275, De Bilt, The Netherlands
- Holland, J.Z., and E.M. Rasmusson, 1973: Measurement of atmospheric mass, energy and momentum budgets over a 500-kilometer square of tropical ocean. *Mon. Wea. Rev.*, **101**, 44-55.
- Kain, J.S., and J. M. Fritsch, 1990: A one-dimensional entraining/detraining plume model and its application in convective parameterization. *J. Atmos. Sci.*, **47**, 2784-2802.
- Neggers, R.A.J., A.P. Siebesma, and H.J.J. Jonker, 2002: A multiparcel method for shallow cumulus convection. *J. Atmos. Sci.*, **59**, 1655-1668.
- Siebesma, A. P., and J.W.M. Cuijpers, 1995: Evaluation of parametric assumptions for shallow cumulus convection. *J. Atmos. Sci.*, **52**, 650-666.
- _____, and A.A.M. Holtslag, 1996: Model impacts of entrainment and detrainment Rates in Shallow Cumulus Convection. *J. Atmos. Sci.*, **53**, 2354-2364.
- _____, 1998: Shallow cumulus convection. *Buoyant Convection in Geophysical Flows*, Vol. 513, E.J. Plate, et al., Eds., Kluwer Academic, 441-486
- _____, et al., 2003: A large eddy simulation intercomparison study of shallow cumulus convection. *J. Atmos. Sci.*, **60**, 1201-1219.
- Stevens, B., and Coauthors, 2001: Simulations of trade wind cumuli under a strong inversion. *J. Atmos. Sci.*, **58**, 1870-1891.
- Tiedtke, M., 1989: A comprehensive mass flux scheme for cumulus parameterization in large-scale models. *Mon. Wea. Rev.*, **117**, 1179-1800.
- Uden, P. et al., 2002: HIRLAM-5 Scientific Documentation, HIRLAM-5 Project, c/o Per Uden SMHI, S-601 76 Norrkoping, Sweden.